47

Invention and Development of Diffusion Tensor MRI (DT-MRI or DTI) at the NIH

PETER J. BASSER

Summay box

This chapter documents the invention and early development of diffusion tensor (DT) NMR and MRI. The author recounts his experiences with his former NIH colleagues, Denis Le Bihan and James Mattiello, from the initial conception of diffusion tensor NMR, to the definition of the apparent diffusion tensor, to the design of the first experiment to measure it. Descriptions of the state of the art in characterizing anisotropic diffusion at the time suggest the significant departure that DT-NMR and DT-MRI represented. Personal recollections and observations are woven through this account of the heady early days of DT-NMR and DT-MRI.

At the time of the invention of DT-MRI (or DTI), I was employed as a Staff Fellow (a postdoctoral fellow position) in the Mechanical Engineering Section (MES) of the Biomedical Engineering and Instrumentation Branch (BEIB) in the Intramural Research Program (IRP) of the National Center for Research Resources (NCRR) of the National Institutes of Health (NIH). (People in the federal government like acronyms!) This was my first postdoctoral position after having graduated from Harvard University's Division of Applied Sciences, where I had studied biofluid and continuum mechanics, and applied mathematics.

Initially, my research activities within BEIB focused on "biomimetics," specifically, the development of models and model systems that mimic more complex biological ones; and studying the response of tissues to impressed mechanical and electric fields. By the early 1990s, my two primary projects involved understanding the physical basis of electromagnetic stimulation (i.e., "magnetic stimulation") of the peripheral (PNS) and central nervous systems (CNS), and understanding the mechanical effects (swelling and consolidation) in the brain during drug infusion.

Bradley Roth (a talented biophysicist and fellow Staff Fellow in the BEIB) and I had developed a mathematical model of magnetic stimulation to explain how induced electromagnetic fields in neural tissue can cause depolarizing or hyperpolarizing transmembrane currents in long axons in the PNS. In one of our papers (Basser and Roth, 1991), we described an axon's trajectory or path as a 3D space curve—a concept that later resurfaced in DTI tractography (Basser, 1998)—while considering the case of magnetic stimulation of an axon whose path is kinked or sinuous. Developing these models of magnetic stimulation led me to realize that we would never be able to determine the action of induced electromagnetic fields on nerves in the CNS or the PNS if we 1) didn't know the coordinates and trajectories of the nerve pathways of interest, and 2) more generally, didn't know the anisotropic and heterogeneous electrical properties (i.e., the

47-Jones-Chap-47.indd 730 8/3/2010 10:47:55 AM

electrical conductivity tensor) of the surrounding tissues in which these nerves are embedded.

In the area of drug delivery and transport, I was fortunate to have been mentored by chemical engineer Bob Dedrick and physical chemist Paul Morrison, who, along with others in the Chemical Engineering Section (CES) in the BEIB had been collaborating with Ed Oldfield, a neurosurgeon at the National Institute of Neurological Disorders and Stroke (NINDS). In the early 1990s, Bob and Paul had proposed a novel drug delivery strategy, later called "convection enhanced delivery" (CED) (Bobo et al., 1994), in which they conceived of infusing drugs (primarily chemotherapeutic agents) directly into the extracellular spaces within the brain near a tumor to overcome the blood–brain barrier that prevented drugs in the bloodstream from ever reaching the tumor. *Convection* refers to the fact that drugs have to be forced into the tissue under pressure and be transported by this mechanism, since diffusion alone often acts too locally to distribute these large drugs effectively. This direct infusion idea was a real breakthrough, but there were attendant problems with getting it to work. One was infusion near or directly into white matter in the brain; the drugs would shoot along white matter tracts rather than spread uniformly near the site of infusion, as they did in many gray matter regions. Bob and Paul wanted to understand this process better and involved me at that point because I had a background in continuum mechanics and porous media theory. We ended up realizing that because the hydraulic permeability of the white matter was so much higher along the fiber tracts than perpendicular to them (i.e., the hydraulic permeability was anisotropic), the prediction of where drugs would eventually migrate and flow required an estimate of the heterogeneous, anisotropic hydraulic permeability (tensor) of brain tissue (Basser, 1992).

My first exposure to diffusion imaging was at a talk that Denis Le Bihan had given on the subject. He had recently come to the NIH from France and was speaking about how diffusion could be used—I think in stroke. While I thought it was very interesting, I didn't make the connection at that time to use diffusion MRI to map anisotropic electrical or hydraulic conductivity tensors in tissue. However, in the early 1990s, Denis Le Bihan and Philippe Douek presented a poster containing very novel and important findings at the annual NIH Research Festival. Denis and Philippe had shown that they could map the nerve fiber direction in different parts of the brain tissue by using the anisotropic properties of water diffusion. That poster was very similar to their previous Society of Magnetic Resonance in Medicine (SMRM) abstract (Douek et al., 1991b). I visited their poster with Brad Roth, and immediately realized first that there was something fundamentally wrong with the mathematical framework they were using to characterize the anisotropic diffusion process in brain tissue. As an aside, it was already well known in the field that water diffusion in the brain was anisotropic (Moseley et al., 1990, 1991), as I later found out. Moseley had even suggested that it was appropriate to use a diffusion tensor to describe this process (Moseley et al., 1991). Denis and Philippe, however, were using a vector model of water diffusion in brain tissue that I knew instinctively had to be described by a diffusion tensor, just the way the hydraulic permeability or electrical conductivities had to be described by a tensor. Denis and Philippe were not alone. Others in the community, as I came to learn, used scalar or vector models of diffusion to describe anisotropic diffusion in the brain. One notable example of a vector method for characterizing features anisotropic diffusion was the work of Richards and colleagues, whose 1992 SMRM abstract was entitled "Vector Analysis of Diffusion Images in Experimental Allergic Encephalomyelitis" (Richards et al., 1992). Filler and colleagues later used the same diffusion-weighted MR signals acquired along only three orthogonal directions as components of a vector to characterize diffusion anisotropy and nerve fiber tracts within the brain (Filler et al., 1993, 1996).

I parked myself in front of Denis and Philippe's poster and began asking Denis innocent questions without tipping my hand, for example, "How do you characterize diffusion in different directions?"; "Aren't there other diffusion components that you have to consider?" At the same time, thoughts were racing through my head about describing this diffusion process with a tensor, which was natural, given my background in continuum mechanics. It wasn't lost on me that a tensor description of a material property provided a tremendous amount of new information.

Frankly, at that point I didn't want to tell Denis what I was thinking, which is maybe a little disingenuous in retrospect, but I think scientists, unfortunately, have to be a little protective, particularly with people whom they don't know.

Afterwards, I raced back to the lab with Brad, almost manically describing to him–while we were walking—the picture of diffusion tensor MRI that was forming in my mind: one could measure not a scalar diffusion coefficient but a diffusion tensor in each voxel, and then calculate the invariants of that tensor and its eigensystem to produce a variety of useful maps and information that didn't appear to be known or available to the MRI community. At that point, my primary interest was still to use the diffusion tensor data to obtain estimates of the hydraulic permeability tensor (for CED) and the electrical conductivity tensor (for magnetic stimulation) by exploiting "cross-properties"—relationships between tensors that describe material properties in different transport processes (e.g., transport of charge, mass, momentum, and energy). Some of this spirit can be seen in the last sentences of the article by Basser, Mattiello, and Le Bihan (1994b).

I worked feverishly for the next few days writing up a prospectus/disclosure that I intended to share with Denis and his NIH colleague, Robert Turner, whom I knew and was friendly with (see Appendix). In this document, I laid out the idea of using the eigenvalues and eigenvectors of the diffusion tensor to provide new features that one could use to form images or maps, the use of the principal invariants of the tensor, such as the trace, determinant, that could provide useful information about tissue properties. I proposed the idea that the eigenvector associated with the largest eigenvalue was the local fiber direction and suggested following fiber tracts as streamlines, using a Mathematica™ figure generated from an analytical (hypothetical) direction-vector field. There was also a representation of a diffusion ellipsoid, also generated in Mathematica™. At the meeting with Denis, Bob Turner, and Brad Roth, I handed out this multi-page document to everyone.

My recollection was that Denis was very excited about it, and quite encouraging, because he knew that this was something that wasn't being done and had real potential. But he said in his—at that time—thick French accent, "There's one problem. You know we don't know how to measure the tensor." I was crestfallen. I came into the meeting full of optimism and left it deeply discouraged. While I had this idea of how to use the diffusion tensor data, I had assumed someone already knew how to measure it! What I had conceived of at that point was a mathematical framework; what was lacking was the NMR physics-based experimental design to supply the data needed for this framework to be used.

The problem was that I knew relatively little NMR physics at that time, having only taken a class on high-resolution spectroscopic NMR methods from Theodore (Ted) Becker a few years before.

At the end of the meeting, Bob and Denis suggested that if I wanted to pursue this problem, I should read some of the classic articles in the diffusion NMR literature, particularly by Stejskal and Tanner. I spent the next few days poring over articles by Stejskal and Tanner, and Carr and Purcell (Carr and Purcell, 1954). In one article by Stejskal (1965), there were a few highly relevant formulas that I needed to understand. I studied one formula in particular in which Stejskal, starting from the Torrey-Bloch equation, related a diffusion tensor to a diffusion-weighted signal, which is discussed further in this book in Chapter 6 by Basser and Özarslan. I set myself to figuring out how we could possibly determine that tensor from measurements of the diffusion-weighted signal, i.e., to invert that equation. After staring at the formula—and it wasn't obvious from the way Stejskal wrote it—I realized that the tensor could be viewed as a matrix that was embedded in a quadratic form, i.e., sandwiched between two vectors that were themselves only related to the parameters of the pulsed-field gradient spin echo experiment. I rewrote this expression in matrix/vector notation and (*Voila*!) realized that this equation was just a simple linear algebraic relationship between the log of the scalar signal that one measured and the projection of the diffusion tensor (obtained along the direction of the applied diffusion gradients). When the quadratic form was expanded, each component of the diffusion tensor was linearly related to the log of the diffusion-weighted signal, i.e., only terms like D_{xx} or D_{xz} appeared, but not terms like $D_{xx} \times D_{xz}$. Then the question I had was, "Could I measure or estimate *all* the components of the tensor from a set of scalar diffusion-weighted data using that equation?" I realized that if one could apply the diffusion gradients in more than three directions (it turned out to be at least six directions), one could obtain enough independent projections of the tensor to be able to "invert" this equation and solve for all of the elements of the tensor. Actually, at the time I had conceived of using multivariate linear regression to estimate each component of the diffusion tensor from the presumably noisy diffusion-weighted signals, which essentially generalized the approach Stejskal and Tanner used to estimate the diffusion coefficient from diffusion-weighted NMR signals. However, at the time, I knew so little about the pulsed-field gradient (PFG) technology that I didn't know whether it was possible or technically feasible to turn on more than one gradient channel at a time to apply a gradient in any direction, so I excitedly wrote Denis an e-mail asking whether one could turn on the x, y, or z components of the diffusion gradient at the same time, rather than only x, y, or z alone. Happily, he replied, "Yes," and I wrote back, "Well in that case then we can measure all of the elements of the tensor!"

The basic diffusion tensor NMR invention then, consisted of the following steps: 1) defining the apparent or the effective diffusion tensor, which was a new MR quantity, 2) relating the apparent diffusion tensor to the diffusion-weighted NMR signal, 3) designing an NMR experiment to measure or estimate this tensor from a set of diffusion-weighted NMR signals, and 4) calculating and displaying new and useful tensor-derived quantities, such as the trace, eigenvalues, eigenvectors, anisotropy measure, tracts, etc.

Figuring out the experimental design for estimating the diffusion tensor was the second "rush" I felt during this invention and development process that was punctuated by the deep disappointment of not knowing how to measure the tensor itself. "Eureka moments" like this make the entire inventive process worthwhile. It's difficult to describe this feeling, but there's a surge of excitement and joy when you figure something out that you have a strong sense may not have been done before and that is potentially very significant. These moments can encourage you to continue to work on and work out problems, often for long periods of time without much success.

As it turns out, this first step was just the beginning of a long journey to develop this new theoretical and experimental design framework for diffusion tensor NMR and in turn for diffusion tensor MRI and then migrate it from bench to bedside.

One person who came on the scene a few weeks later was James Mattiello, who was also a Staff Fellow in the BEIB. The financial support for the project he was hired to work on had dried up and he was looking for new projects. One, I think, was with Denis to image temperature in the body using diffusion MRI. Jim approached me, wanting to work on diffusion tensor MR measurements, which he must have heard about from his discussions with Denis. I was excited about this prospect because Jim already had a good technical background in diffusion MRI, and he would provide a lot of experimental know-how and support for the early validation and testing studies that we needed to perform. Frankly, I couldn't perform these on my own because of my limited knowledge of NMR hardware and pulse sequence programming.

Denis arranged magnet time for us at the *In Vivo* NMR Center, now the NIH MRI Research Facility (NMRF: http://intranet.nmrf.nih.gov/) on a 4.7T spectrometer/imaging (GE Fremont, CA), now long retired. With the DT-NMR mathematical framework and experimental design in hand, the first task was to show that the diffusion tensor in water was an isotropic second-order tensor. This means that if you look at the diffusion process along any direction you'll measure the same diffusivity. If you can't demonstrate this, you can't hope to apply this method to anisotropic tissues, like brain white matter or skeletal muscle. Initially, Jim and I began doing these diffusion tensor NMR experiments with water and glycerin phantoms. We continued these experiments for a long time because we weren't able to show initially, and for quite some time thereafter, within the experimental error, that these isotropic liquids produced isotropic diffusion tensors.

After a time, I started to make regular trips to the local Safeway to buy pork loin and cow hearts to use as NMR phantoms. Jim, who had come from an Italian-American background, recommended spaghetti squash as a possible NMR phantom, which, because of its stringiness, would exhibit anisotropic diffusion properties. The pork loin and water experiments were summarized in our first SMRM abstracts on DT-NMR that appeared in 1992 (Basser and Le Bihan, 1992; Basser et al., 1992).

In fact, in the 1970s, various investigators (Hansen, 1971; Rorschach et al., 1973; Hazlewood et al., 1974; Cleveland et al., 1976; Tanner, 1979) had already looked at diffusion anisotropy in skeletal muscle and in other tissues, but they didn't measured the diffusion tensor the way we did. First, they didn't use a tensor framework to study it. They all presumed that they could orient the tissue in the magnet so that the fiber direction could be aligned perfectly along the direction of their magnetic field gradient to obtain the diffusivity along the main axis of the fibers. Then they could rotate the sample so that the fibers were perpendicular to the same *diffusion gradient* in order to measure a transverse diffusivity. Since tissues are optically turbid, one can't determine by visual inspection how their fibers are aligned, so it is preferable to determine the directions of maximum and minimum diffusivity using the NMR experiment itself for this purpose. Moreover, the

DT-NMR experimental design didn't require moving the sample within the magnet but instead allowed a specimen to remain stationary in the magnet, using the *x*-, *y*- and *z*-gradients to change the direction of the diffusion-sensitizing gradients applied to the specimen. Our first SMRM (now ISMRM) abstracts (Basser and Le Bihan, 1992; Basser et al., 1992) recapitulated findings from these earlier diffusion NMR experiments using our new diffusion tensor NMR methodology. We took a macroscopically uniform slab of pork loin and measured the diffusion tensor within a large excited volume. Then we physically rotated that specimen in the magnet. We repeated the entire DT-NMR experiment and recalculated the tensor. We were able to show that the change in fiber direction (i.e., the eigenvector associated with the largest eigenvalue) that we measured in the pork loin by NMR corresponded to the direction in which we rotated the specimen! We also showed that, despite the physical rotation of the specimen, the invariants of the diffusion tensor, like the trace, and the eigenvalues or principal diffusivities hardly changed, showing that these were truly intrinsic to the tissue.

We continued to measure the diffusivity in water because we were still unable to observe true isotropic diffusion in this phantom to within a few percent. In fact, this is discussed in our later paper (Basser et al., 1994b). For a long time, we were trying to figure out what artifact(s) might be causing this deviation from isotropy. The recognition of the exquisite sensitivity of the diffusion tensor measurement to features of the pulsed-field gradient waveform actually led us to another idea, which became part of our first patent disclosure, i.e., to use the diffusion tensor MR measurement in a phantom with known diffusion properties in order to calibrate MR gradients (Basser et al., 1996).

In fact, Denis had pointed out to me much earlier that the diffusion sensitization—the attenuation of the diffusion signal—went with the square of the diffusion gradient strength, whereas the phase signal only scales with the gradient strength to the first power. Therefore, the diffusion signal is much more sensitive to the gradient value than the phase, and this could be used as a way of calibrating the gradients. It occurred to me that the same idea could be applied in 3D using the diffusion tensor experiment. If we know that water is isotropic and we're not measuring an isotropic tensor, why don't we use that disparity to recalibrate the gradient system to essentially equalize and orthogonalize them in software, so that the measured tensor will now have the correct isotropic form and have the correct diffusivity at the ambient temperature? In this way, we could conceivably correct systematic errors. For this correction I also worked out the theory that we eventually included in our patent application (Basser et al., 1996) but never published as a journal article.

The next step was to migrate the diffusion tensor NMR experiment to a diffusion tensor MRI experiment for eventual translation from bench to beside. Denis was probably *the* world expert on clinical diffusion MRI, having worked out the first clinically feasible sequence for doing it, and thoroughly understood the DWI pulse sequences and the importance of calculating and accounting for "cross-terms" that arise. To do DT-MRI we now needed to calculate every element of the b-matrix, the diffusion MRI analog of the *b*-value, for much more complicated DWI experiments than the DW-NMR experiments we had performed previously. The b-matrix turned out to be a much more complicated object, since in order to compute all its elements, one had to use all three (i.e., *x*-, *y*-, and *z*-) gradient waveforms. Arriving at analytical expressions for all the b-matrix elements for the 2D FT spin echo DW MRI (see Mattiello et al., 1994) sequence and later the DW echo-planar MRI sequence (see Mattiello et al., 1997) consumed quite a bit of Jim Mattiello's time while at the NIH. I passed off my Mathematica™ code for doing the analytical b-matrix calculations to Jim to get him started developing the analytical expressions for the b-matrices for DWI sequences. Jim worked assiduously in the *In Vivo* NMR Center to advance DT-MRI (Basser et al., 1994a; Mattiello et al., 1995).

Jim and Denis were wonderful collaborators. We all worked hard and worked well together, and we were beginning to produce interesting findings using this new DT-NMR and later the DT-MRI experiments. Working with Peter Jezzard, we were even able to obtain a diffusion ellipse image on a live human brain, which was included as a figure in Denis' excellent book on perfusion and diffusion imaging (Le Bihan, 1995). So, it shouldn't be too surprising that I was deeply disappointed to learn that both Jim and Denis were planning to leave the NIH within a few months of each other—Denis to take an excellent job in the French Atomic Energy Commission (CEA), and Jim to become an entrepreneur with plans to found a start-up robotics company in Michigan. In the aftermath, I wondered whether we would ever bring DT-MRI from bench to bedside.

Luckily, people in the field, with the exception of maybe one or two groups, such as Mark Horsfield's in Leicester, largely overlooked our DT-NMR and MRI work. I've heard subsequently from several colleagues that they found our articles too mathematical or too intimidating to implement. Although this is an apocryphal story, it was relayed to me that a graduate student working at Massachusetts General Hospital, one of the top radiology research programs in the world, apparently was discouraged from doing his thesis on DT-MRI because his thesis advisor thought it had no clinical potential.

Happily, it turned out that just around the time Jim and Denis left I met an Italian post-doctoral researcher named Carlo Pierpaoli, who had recently come to the NINDS from Georgetown University, where he studied the effects of benzodiazepines and other drugs on the brain. He had already begun doing diffusion MRI experiments at the NIH and was interested in DT-MRI. He approached me, if I recall, about the possibility of working together. I was a little leery at first, because I didn't know much about him, but the more time I spent with him the more I realized he was a brilliant and serious person who was learning the DTI technology very quickly. As time progressed, we started to work very closely together. Carlo began expanding upon Jim Mattiello's IDL code and began to adapt it for in vivo biological and clinical applications.

Carlo's background in neurology turned out to be exceptionally helpful. Over time, developing DTI for clinical applications really became his major research focus. At the NINDS, Carlo worked with Alan Barnett, a talented physicist who began developing 2D Fourier transform diffusion-weighted spin echo MRI sequences that would allow you to do these DTI experiments in sedated monkeys. Working with Alan and then eventually with Peter Jezzard, Carlo created an infrastructure to acquire diffusion-weighted echo-planar MRIs with high enough spatial resolution and high enough image quality to be able to do DT-MRI first in sedated monkeys and then ultimately in humans (Pierpaoli et al., 1996). So I think a large part of the early bench-to-bedside migration was due to Carlo's coaching and effort and his involvement in that project. The MRI physics input was primarily from Alan Barnett and Peter Jezzard.

It became clear to me that for the field to advance, we would have to develop simple scalar descriptors of the diffusion process

that clinicians and biologists could use to interpret the complicated DTI data. This was the impetus for defining different measures of diffusion anisotropy and producing maps of them (Basser, 1995; Basser and Pierpaoli, 1996). This work resulted in the proposal of the fractional anisotropy (FA) and relative anisotropy as indices of diffusion anisotropy. Carlo independently arrived at a definition for the volume ratio. These quantities had the useful feature that they were intrinsic to the tissue, were orientationally invariant, and provided a quantitative assessment of the degree of "out of roundness" of the diffusion ellipsoid.

Following Carlo's *Radiology* paper (Pierpaoli et al., 1996), there appeared to be flat growth in the DTI field. Many people apparently still didn't understand how to measure a tensor. They didn't understand what it was, what new information it provided, except for a few groups. We realized that we had to make DTI more accessible. Unfortunately, some of our early papers, particularly those about the analytical computation of b-matrices, may have put many people off, making DTI appear needlessly complicated.

I realized that we had to reduce the "activation barrier" for implementing DTI, making it simpler and more accessible to people who otherwise wouldn't try it. To this end, I went back to a special case we considered in our article on tensor estimation (Basser et al., 1994a), in which we suggested that only seven diffusion-weighted signals could be used to obtain an analytical expression for the diffusion tensor. We showed a simple way to perform DTI by acquiring seven diffusion-weighted signals in each voxel and presented simple formulas to calculate each element of the diffusion tensor and even a few important tensor-derived quantities (Basser and Pierpaoli, 1998) from the diffusion-weighted signals. In an afternoon, one could acquire the necessary DWI data and perform a complete DTI analysis using an Excel spreadsheet.

In fact, shortly thereafter, General Electric Medical Systems picked up on our "simplified method" and started distributing it to its research sites as an add-on to its FuncTool package. Perhaps for the first time, people realized that DTI was straightforward to implement and that one didn't need to be a rocket scientist to do it. One could take the original DWI data and calculate the tensor and then calculate all of these useful parameters like the trace, and the fiber directions, and make FA maps and display the other features that we had already presented and talked about. Actually, a number of people have told me that before that paper came out, they were really not interested in doing DTI. Happily, following its publication there was another up tick in interest in the subject and people started using it more and more.

Soon, many clinical programs had access to the DTI technology because it was provided either by physicists in their programs or through the commercial sequences and analysis tools that companies began providing. Subsequently, there was a surge in clinical applications. In the clinical or "bedside" phase, studies started to appear that applied DTI to characterize many different diseases and disorders.

It is probably valuable at this point to backtrack a bit to discuss the issues relating to the invention and development of DTI tractography, which has now become a separate field. As described earlier, there were several groups who were developing methods for visualizing fiber orientation in the brain. I believe one novel concept we contributed in our 1994 article was the notion that DT-MRI provided a means "of visualizing muscle and nerve fiber tracts individually" (Basser et al., 1994b). In that article we had also introduced the notion that the principal direction of the diffusion tensor associated with the largest eigenvalue within a voxel provided a local estimate of the fiber orientation in coherent fiber bundles. While we may have conceived of DTI tractography, we didn't present an algorithm to "reduce it to practice" at that time. I think that distinction goes to Van Wedeen, whose abstracts presented at meetings of the Organization for Human Brain Mapping (Wedeen et al., 1995, 1996) (unbeknownst to me) provided two different algorithms for performing DTI tractography.

Regarding the depiction of tracts, Carlo Pierpaoli and Sinisa Pajevic came up with a very compelling way of displaying local fiber tract orientation using color. Carlo and Sinisa realized that one could color code the eigenvector associated with the largest eigenvalue encoding the x, y, and z components, using red, green, and blue, respectively (Pierpaoli, 1997; Pajevic and Pierpaoli, 1999, 2000). Around the same time, Derek Jones did this as well (Jones et al., 1997). By combining this color-encoding scheme with an image that is essentially a filter for white matter, such as the FA, a direction-encoded color (DEC) map of the brain could be made, where one could see the local direction of the fiber by looking at the color.

While Philippe and Denis had actually proposed a novel color scheme previously (Douek et al., 1991a, 1991b), Carlo's and Sinisa's was based on the fiber orientation calculated from DTI data (i.e., the eigenvector of the diffusion tensor associated with the largest eigenvalue), and assigned a color to it that was related to its orientation in the laboratory or patient's frame of reference. This innovation has turned out to be a very powerful way of looking at white matter pathways. In fact, Carlo and Sinisa showed that, using this method, they could identify the primary white matter pathways in the brain (i.e., projection, commissural, and association fibers) (Pajevic and Pierpaoli, 1999, 2000). It was from seeing these DEC maps and learning how to interpret them that I had the confidence and impetus to finally develop algorithms to perform DTI tractography. Prior to seeing these images, the idea of doing DTI tractography on noisy, sparse brain image data seemed far-fetched. However, toward the end of the 1990s, the quality and resolution of DWIs and, hence, DTI brain data had improved markedly. Maybe it was time to revisit this problem.

This apparently was on the mind of other scientists like Poupoun (Poupon et al., 1998), Mori (Mori et al., 1999), Conturo (Conturo et al., 1999), and Jones (Jones et al., 1997, 1999) as well as others who were developing methods to perform tractography.

My approach to DTI tractography was to represent the computed tracts as though they were fluid streamlines. Since my background was in fluid mechanics, this was quite natural. The trick was that we had to construct a streamline from a discrete estimate of the normalized tangent vector to the purported fiber tract bundle. The key idea here was to represent the streamline or tract path as a 3D space curve, whose normalized tangent vector was parallel to the eigenvector associated with the largest eigenvalue. The Frenet equations describing the evolution of the 3D space curve are differential equations that needed to be solved to generate a tract trajectory. The problem was that because we only measure discrete DTI data, solving such a set of differential equations required a way to interpolate or approximate the diffusion tensor field continuously within the imaging volume.

The development of a method for continuously approximating a noisy, discretely sampled tensor field was primarily due to Akram Aldroubi, who had worked in the BEIB with me previously. He developed the mathematical machinery to do this tensor field approximation in a fast and efficient manner using

B-splines, based on an elegant theory of tensor approximations he proposed (Aldroubi and Basser, 1999). Sinisa Pajevic implemented Akram's mathematical framework to produce the software to be able to essentially weave together these discrete tensor measurements into a continuous tensor fabric or field that one could follow seamlessly through the brain (Pajevic et al., 2002). Once that fabric was created, it was a simple task to solve the differential equation for one of these fiber tracts or strands.

The diffusion MRI field has advanced in so many exciting and wonderful ways since our early work in DTI. What is still remarkable to me is that as we look forward to addressing important biological and clinical problems as well as applications in neurosciences, water displacement–based imaging methods still offer so many possibilities for future development!

As a closing statement, I hope that no one who reads this account feels slighted for what he or she believes to be his or her original contributions to the field of DTI. This account represents only my personal recollection of events related to the invention and development of DTI.

Appendix

Peter J. Basser 1 11/19/91

DEPARTMENT OF HEALTH & HUMAN SERVICES — Public Health Service, National Institutes of Health

Memorandum

Date: Original: November 11, 1991
Revised: November 14, 1991
Revised: November 19, 1991

Meeting copy

To: Denis LeBihan
Philip Douek
Bob Turner
Brad Roth

From: Peter Basser, BEIP, NCRR

Re: Diffusivity/Anisotropy Imaging

Goal: To use the self-diffusion tensor measured MRI[1] to:

a) measure and/or monitor the "para" and "ortho" diffusivities in anisotropic media, such as white matter or heart tissue *in vivo*, or in non-biological materials

b) measure and/or monitor the fiber orientation in anisotropic media, such as white matter or heart tissue *in vivo*, or in non-biological materials.

c) diagnose diseases that may be associated with pathological changes in diffusivity like MS and/or anatomy such as IHHS.

[1] or some other non-invasive imaging modality, such as EPR or ESR,

Proposed Methods:

a) Determine the three principal axes, $\varepsilon_1[i]$, $\varepsilon_2[i]$, $\varepsilon_3[i]$ (eigenvectors) of the diffusivity tensor and their corresponding eigenvalues, $\lambda_1[i]$, $\lambda_2[i]$, $\lambda_3[i]$ in each voxel (denoted by the index [i]). If $\underline{D}[i]$ is the diffusivity tensor in voxel i, e.g.,

$$\underline{D}[i] = \begin{matrix} 2 & 1 & 0 \\ 1 & 2 & 1 \\ 0 & 1 & 2 \end{matrix}$$

then its eigenvalues and corresponding eigenvectors are:

$$\lambda_1[i] = 2+\sqrt{2}, \quad \Leftrightarrow \quad \varepsilon_1[i] = \{\frac{1}{2}, \frac{1}{\sqrt{2}}, \frac{1}{2}\}^T,$$

$$\lambda_2[i] = 2, \quad \Leftrightarrow \quad \varepsilon_2[i] = \{\frac{-1}{\sqrt{2}}, 0, \frac{1}{\sqrt{2}}\}^T,$$

$$\lambda_3[i] = 2-\sqrt{2}, \quad \Leftrightarrow \quad \varepsilon_3[i] = \{\frac{-1}{2}, \frac{1}{\sqrt{2}}, \frac{-1}{2}\}^T.$$

In each voxel the eigenvalues of the diffusivity tensor are ordered with $\lambda_1[i]$ being the largest and $\lambda_3[i]$ being the smallest. The eigenvalues represent the "para" and "ortho" diffusivities, i.e.,

$$\lambda_1[i] = D[i]_{para}$$

$$\lambda_2[i] = D[i]_{ortho1}$$

$$\lambda_3[i] = D[i]_{ortho2}$$

The eigenvectors of $\underline{D}[i]$, $\varepsilon_1[i]$, $\varepsilon_2[i]$, and $\varepsilon_3[i]$, point in the "para" and "ortho" directions relative the coordinate system in which the diffusivity tensor was originally measured. The diffusivity tensor is now diagonalized by adopting a coordinate system aligned with the "ortho" and "para" directions. This entails a transformation of a vector in the laboratory frame, $\mathbf{X}[i]$, to the local fiber frame, $\mathbf{Z}[i]$, by:

$\mathbf{Z}[i] = \underline{E}[i]^T (\mathbf{X}[i] - \mathbf{A}[i])$ { for simplicity we'll call this $\mathbf{z}[i] = \underline{E}[i]^T \mathbf{x}[i]$ }

where $\underline{E}[i]$ is the matrix whose columns are the normalized eigenvectors of $\underline{D}[i]$, i.e.,

$$\underline{E}[i] = \left(\frac{\varepsilon_1[i]}{|\varepsilon_1[i]|} \; \Big| \; \frac{\varepsilon_2[i]}{|\varepsilon_2[i]|} \; \Big| \; \frac{\varepsilon_3[i]}{|\varepsilon_3[i]|} \right)$$

and $\mathbf{A}[i]$ is the vector from the origin of the lab frame to the center of voxel i.

The diagonal matrix, $\underline{\Delta}[i]$, whose elements are

$$\underline{\Delta}[i] = \begin{matrix} \lambda_1[i] & 0 & 0 \\ 0 & \lambda_2[i] & 0 \\ 0 & 0 & \lambda_3[i] \end{matrix}$$

is related to $\underline{D}[i]$ by

$$\underline{D}[i] = \underline{E}[i] \, \underline{\Delta}[i] \, \underline{E}[i]^T$$

b) Construct a 3-D vector plot of the $\varepsilon_1[i]$ s corresponding to $\lambda_1[i] = D[i]_{para}$ for each voxel. Recall, $\varepsilon_1[i]$ defines the "para" direction of the fibers in a particular voxel. An example of a 3D vector plot is given below:

47-Jones-Chap-47.indd 736 8/3/2010 10:47:56 AM

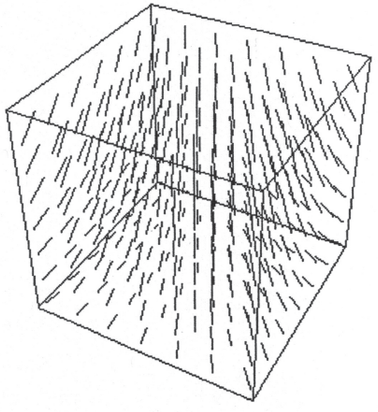

what happens when preferred direction

Projections of the principal eigenvector in a particular plane could be viewed as well.

c) Use 3D plotting routines to display the *mean diffusion ellipsoid* - the quadratic forms, $\mathbf{Z}[i]^T \underline{\Delta}[i]^{-1} \mathbf{Z}[i] = 2\,c$, derived from the diffusivity tensor in each voxel. In the transformed coordinate system, this quadratic form takes on the simple form:

$$\frac{x[i]^2}{\lambda_1[i]} + \frac{y[i]^2}{\lambda_2[i]} + \frac{z[i]^2}{\lambda_3[i]} = 2\,c$$

or

$$\left(\frac{x[i]}{\sqrt{2\lambda_1[i]\,c}}\right)^2 + \left(\frac{y[i]}{\sqrt{2\lambda_2[i]\,c}}\right)^2 + \left(\frac{z[i]}{\sqrt{2\lambda_3[i]\,c}}\right)^2 = 1$$

and may appear as

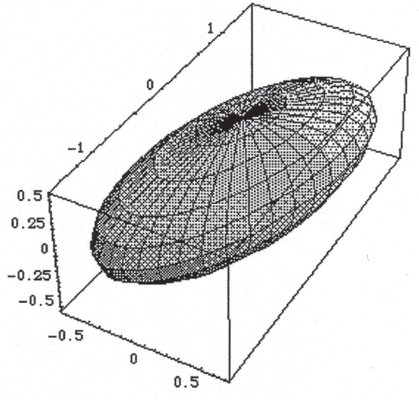

The major and minor axes of this ellipsoid are coincident with the eigenvectors of $\underline{D}[i]$; their lengths are proportional to the square roots of the eigenvalues of $\underline{D}[i]$, $\sqrt{\lambda_j[i]}$. We can ascribe a physical interpretation to the shape of the ellipsoid. Since the *mean* diffusion distance in the j^{th} principal direction, δ_j, is given approximately by

$$\delta_j[i] \approx \sqrt{2\lambda_j[i]\,c}$$

the magnitudes of the major axes of the ellipsoid are just the average distances that the diffusing species travels in the three principal directions in time c from an initial point distribution at the voxel's center at t=0.

To see this we need to solve the anisotropic diffusion equation. We combine Fick's Law of diffusion for an anisotropic medium,

$$\mathbf{J} = -\underline{D}\,\nabla C\,,$$

really want Block eq with convection & diffusion

with the equation of conservation of mass of the solute,

$$\frac{\partial C}{\partial t} = -\nabla \bullet \mathbf{J}\,.$$

Substituting the first equation into the second we get,

47-Jones-Chap-47.indd 737 8/3/2010 10:47:59 AM

$$\frac{\partial C}{\partial t} = \nabla \bullet \left(\underline{D}\, \nabla C\right) = D_{ij} \frac{\partial^2 C}{\partial x_i \partial x_j}$$

where the Einstein summation convention is used. If a point source at the center of voxel i, has an initial magnetization distribution, M $\delta(\mathbf{x}[i])\ \delta(t)$, the concentration of aligned particles should be given by:

$$C(\mathbf{x}[i], t) = \frac{M}{\sqrt{|\underline{D}[i]|}(4\pi t)^{3/2}} \mathrm{Exp}\left(\frac{-\,\mathbf{x}[i]^T\, \underline{D}[i]^{-1}\, \mathbf{x}[i]}{4t}\right) .$$

This is a complicated expression with a high degree of coupling among the three coordinate direction in the lab frame. Using the relationship: $\underline{D}[i] = \underline{E}[i]\ \underline{\Delta}[i]\ \underline{E}[i]^T$, we see that

$$C(\mathbf{x}[i], t) = \frac{M}{\sqrt{|\underline{D}[i]|}(4\pi t)^{3/2}} \mathrm{Exp}\left(\frac{-\,\mathbf{x}[i]^T\, (\underline{E}[i]\ \underline{\Delta}[i]\ \underline{E}[i]^T)^{-1}\, \mathbf{x}[i]}{4t}\right).$$

Using the relations:

$$\underline{D}[i]^{-1} = \left(\underline{E}[i]\ \underline{\Delta}[i]\ \underline{E}[i]^T\right)^{-1} = \underline{E}[i]\ \underline{\Delta}[i]^{-1}\ \underline{E}[i]^T ,$$

applicable for the unitary matrix E[i], and regrouping terms in the exponent:

$$C(\mathbf{x}[i], t) = \frac{M}{\sqrt{|\underline{D}[i]|}(4\pi t)^{3/2}} \mathrm{Exp}\left(\frac{-\,(\mathbf{x}[i]^T\, \underline{E}[i])\ \underline{\Delta}[i]^{-1}\ (\underline{E}[i]^T\, \mathbf{x}[i])}{4t}\right)$$

substituting $\mathbf{z}[i] = \underline{E}[i]^T\, \mathbf{x}[i]$ and $\mathbf{z}[i]^T = \mathbf{x}[i]^T\, \underline{E}[i]$, and $|\ \underline{D}[i]\ | = |\ \underline{\Delta}[i]\ |$ we get:

$$C(\mathbf{z}[i], t) = \frac{M}{\sqrt{|\underline{\Delta}[i]|}(4\pi t)^{3/2}} \mathrm{Exp}\left(\frac{-\,\mathbf{z}[i]^T\, \underline{\Delta}[i]^{-1}\, \mathbf{z}[i]}{4t}\right).$$

We have sucessfully decoupled diffusion fluxes into their three principal directions.

We can use this solution to generate families of ellipsoids that are actually surfaces of equal concentration obtained by setting the exponent above to different positive constants, β,

$$\mathbf{z}[i]^T\, \underline{\Delta}[i]^{-1}\, \mathbf{z}[i] = \beta .$$

The quadratic form defining the mean diffusion ellipsoid is just a special case in which $\beta = 4t$, so at any time t, its perimeter encompasses one standard deviation of the Gaussian concentration distribution in each of the three principal directions.

When all the ellipsoids for each voxel are displayed together they resemble link sausages that follow the fiber tracks.

d) Compute the three invariants of the diffusion tensor in each voxel:

$$I_1[i] = \lambda_1[i] + \lambda_2[i] + \lambda_3[i] = \mathrm{Tr}\,\underline{D} = \mathrm{Tr}\,\underline{\Delta}$$

$$I_2[i] = \lambda_1[i]\,\lambda_2[i] + \lambda_3[i]\,\lambda_1[i] + \lambda_2[i]\,\lambda_3[i]$$

$$I_3[i] = \lambda_1[i]\,\lambda_2[i]\,\lambda_3[i] = |\,\underline{D}\,| = |\,\underline{\Delta}\,|$$

These numbers are intrinsic to the diffusion tensor and are independent of the specific coordinate system used to represent it and fiber directions. Therefore, they may provide useful clinical or structural information when they are compared with the same quantities computed in other voxels of the same patient or with corresponding voxels of other patients.

e) Construct ratios of the eigenvalues or diffusivities in each voxel:

$$\frac{\lambda_1[i]}{\lambda_2[i]} = \frac{D[i]_{para}}{D[i]_{ortho1}} ; \quad \frac{\lambda_1[i]}{\lambda_3[i]} = \frac{D[i]_{para}}{D[i]_{ortho2}}$$

These ratios measure the degree of rotational symmetry about the major axis and the relative magnitudes of the "para" and two "ortho" diffusivities. They may change in diseases like MS. Approximations to these quantities are currently being computed by Douek et al.

Onsager's relationships from non-equilibrium thermodynamics require that the diffusion tensor is symmetric, i.e., $\underline{D}[i] = \underline{D}[i]^T$, implying that its eigenvalues are all real and its eigenvectors are all orthogonal. All the eigenvalues also must be positive, otherwise diffusion in at least one

47-Jones-Chap-47.indd 738 8/3/2010 10:48:00 AM

Peter J. Basser 8 11/19/91

direction would increase the magnitude of concentration gradients rather than reduce them, violating the second law of thermodynamics. In other words, the diffusivity tensor is also positive definite. These constraints can be used to pre-process the measured diffusion tensor. Before performing this principal component analysis we can symmetrize the tensor

$$\underline{D}[i] = \frac{1}{2}\left(\underline{D}[i]_{measured} + \underline{D}[i]_{measured}^{T}\right) .$$

In addition, these conditions can help in quality assurance of the measurement system.

The effect of measurement error on the eigenvalues and eigenvectors of $\underline{D}[i]$ can be ascertained using Monte Carlo simulations once the distribution from which the components of $\underline{D}[i]$ and its statistical parameters are determined experimentally.

Sophisticated image processing procedures can be applied to integrate the vector field in order to interpolate the fiber orientations between voxels.

Submitted by: Peter Basser

References

Aldroubi A, Basser PJ (1999). Reconstruction of vector and tensor fields from sampled discrete data. In Baggett LW, Larson DR (Eds.), *Contemporary Mathematics*. Providence, RI: AMS.

Basser PJ (1992). Interstitial pressure, volume, and flow during infusion into brain tissue. *Microvasc Res* 44(2):143–165.

Basser PJ (1995). Inferring microstructural features and the physiological state of tissues from diffusion-weighted images. *NMR Biomed* 8(7-8):333–344.

Basser PJ (1998). Fiber-tractography via diffusion tensor MRI (DT-MRI). Paper read at 6th Annual Meeting of the ISMRM, April 18–24, 1998, Sydney, Australia.

Basser PJ, Le Bihan D (1992). Fiber orientation mapping in an anisotropic medium with NMR diffusion spectroscopy. Paper read at the 11th Annual Meeting of the SMRM, Berlin.

Basser PJ, Mattiello J, Le Bihan D (1992). Diagonal and off-diagonal components of the self-diffusion tensor: their relation to and estimation from the NMR spin-echo signal. Paper read at the 11th Annual Meeting of the SMRM, Berlin.

Basser PJ, Mattiello J, Le Bihan D (1994a). Estimation of the effective self-diffusion tensor from the NMR spin echo. *J Magn Reson B* 103(3): 247–254.

Basser PJ, Mattiello J, Le Bihan D (1994b). MR diffusion tensor spectroscopy and imaging. *Biophys J* 66(1):259–267.

Basser PJ, Mattiello J, Le Bihan D (1996). Method and system for measuring the diffusion tensor and for diffusion tensor imaging. Bethesda, MD: National Institutes of Health.

Basser PJ, Pierpaoli C (1996). Microstructural and physiological features of tissues elucidated by quantitative-diffusion-tensor MRI. *J Magn Reson B* 111(3):209–219.

Basser PJ, Pierpaoli C (1998). A simplified method to measure the diffusion tensor from seven MR images. *Magn Reson Med* 39(6):928–934.

Basser PJ, Roth BJ (1991). Stimulation of a myelinated nerve axon by electromagnetic induction. *Med Biol Eng Comput* 29(3):261–268.

Bobo RH, Laske DW, Akbasak A, Morrison PF, Dedrick RL, Oldfield EH (1994). Convection-enhanced delivery of macromolecules in the brain. *Proc Natl Acad Sci U S A* 91(6):2076–2080.

Carr HY, Purcell EM (1954). Effects of diffusion on free precession in nuclear magnetic resonance experiments. *Phys Rev* 94(3):630–638.

Cleveland GG, Chang DC, Hazlewood CF, Rorschach HE (1976). Nuclear magnetic resonance measurement of skeletal muscle: anisotropy of the diffusion coefficient of the intracellular water. *Biophys J* 16(9): 1043–1053.

Conturo TE, Lori NF, Cull TS, Akbudak E, Snyder AZ, Shimony JS, McKinstry RC, Burton H, Raichle ME (1999). Tracking neuronal fiber pathways in the living human brain. *Proc Natl Acad Sci U S A* 96 (18):10422–10427.

Douek P, Turner R, Pekar J, Patronas N, Le Bihan D (1991a). MR color mapping of myelin fiber orientation. *J Comput Assist Tomogr* 15 (6): 923–929.

Douek P, Turner R, Pekar J, Petronas N, Le Bihan D (1991b). Myelin fiber orientation color mapping. Paper read at the 10th Annual Conference of the SMRM, San Francisco.

Filler AG, Howe FA, Hayes CE, Kliot M, Winn HR, Bell BA, Griffiths JR, Tsuruda JS (1993). Magnetic resonance neurography. *Lancet* 341(8846):659–661.

Filler AG, Tsuruda JS, Richards TL, Howe FA (1996). *Image Neurography and Diffusion Anisotropy Imaging*, edited by U. S. P. a. T. Office.

Hansen JR (1971). Pulsed NMR study of water mobility in muscle and brain tissue. *Biochim Biophys Acta* 230(3):482–486.

Hazlewood CF, Chang DC, Nichols BL, Woessner DE (1974). Nuclear magnetic resonance transverse relaxation times of water protons in skeletal muscle. *Biophys J* 14(8):583–606.

Jones DK, Simmons A, Williams SC, Horsfield MA (1999). Non-invasive assessment of axonal fiber connectivity in the human brain via diffusion tensor MRI. *Magn Reson Med* 42(1):37–41.

Jones DK, Williams SCR, Horsfield MA (1997). Full representation of white-matter fibre direction on one map via diffusion tensor analysis. Paper read at the 5th Annual ISMRM Meeting, Vancouver.

Le Bihan D (1995). *Diffusion and Perfusion Magnetic Resonance Imaging*. New York: Raven Press.

Mattiello J, Basser PJ, Le Bihan D (1994). Analytical expression for the b-matrix in NMR diffusion imaging and spectroscopy. *J Magn Reson A* 108:131–141.

Mattiello J, Basser PJ, Le Bihan D (1995). Analytical calculation of the b matrix in diffusion imaging. In Le Bihan D (Ed.), *Diffusion and Perfusion Magnetic Resonance Imaging*. New York: Raven Press.

Mattiello J, Basser PJ, Le Bihan D (1997). The b-matrix in diffusion tensor echo-planar imaging. *Magn Reson Med* 37(2):292–300.

Mori S, Crain BJ, Chacko VP, van Zijl PC (1999). Three-dimensional tracking of axonal projections in the brain by magnetic resonance imaging. *Ann Neurol* 45(2):265–269.

Moseley ME, Cohen Y, Kucharczyk J, Mintorovitch J, Asgari HS, Wendland MF, Tsuruda J, Norman D (1990). Diffusion-weighted MR imaging of anisotropic water diffusion in cat central nervous system. *Radiology* 176(2):439–445.

Moseley ME, Kucharczyk J, Asgari HS, Norman D (1991). Anisotropy in diffusion-weighted MRI. *Magn Reson Med* 19(2):321–326.

Pajevic S, Aldroubi A, Basser PJ (2002). A continuous tensor field approximation of discrete DT-MRI data for extracting microstructural and architectural features of tissue. *J Magn Reson* 154(1):85–100.

Pajevic S, Pierpaoli C (1999). Color schemes to represent the orientation of anisotropic tissues from diffusion tensor data: application to white matter fiber tract mapping in the human brain. *Magn Reson Med* 42(3): 526–540.

Pajevic S, Pierpaoli C (2000). Color schemes to represent the orientation of anisotropic tissues from diffusion tensor data: application to white matter fiber tract mapping in the human brain. *Magn Reson Med* 43(6):921.

Pierpaoli C (1997). Oh no! One more method for color mapping of fiber tract direction using diffusion MR imaging data. Paper read at the 5th Annual Meeting of ISMRM, Vancouver.

Pierpaoli C, Jezzard P, Basser PJ, Barnett A, Di Chiro G. (1996). Diffusion tensor MR imaging of the human brain. *Radiology* 201(3):637–648.

Poupon C, Mangin J-F, Frouin V, Regis F, Pachot-Clouard M, Le Bihan D, Bloch I (1998). Regularization of MR diffusion tensor maps for tracking brain white matter bundles. Paper read at Proceedings of MICCAI '98, MIT, Boston.

Richards TL, Heide AC, Tsuruda JS, Alvord ES (1992). Vector analysis of diffusion images in experiment[al] allergic encephalomyelitis. Paper read at the Society of Magnetic Resonance in Medicine, Berlin.

Rorschach HE, Chang DC, Hazlewood CF, Nichols BL (1973). The diffusion of water in striated muscle. *Ann N Y Acad Sci* 204:444–458.

Stejskal EO (1965). Use of spin echoes in a pulsed magnetic-field gradient to study anisotropic restricted diffusion and flow. *J Chem Phys* 43(10): 3597–3603.

Tanner JE (1979). Self-diffusion of water in frog muscle. *Biophys J* 28(1): 107–116.

Wedeen VJ, Davis TL, Lautrup BE, Reese TG, Rosen BR (1996). Diffusion anisotropy and white matter tracts. Paper read at the Proceedings of the Second International Conference for Functional Mapping of the Human Brain, Boston.

Wedeen VJ, Davis TL, Weisskoff RM, Tootell R, Rosen BR, Belliveau JW (1995). White matter connectivity explored by MRI. Paper read at Proceedings of the First International Conference for Functional Mapping of the Human Brain, Paris.